ЯДЕРНА ФІЗИКА
NUCLEAR PHYSICS

УДК 539.142 https://doi.org/10.15407/jnpae2020.02.113

S. Shlomo[1], A. I. Sanzhur[2,*]

[1] *Cyclotron Institute, Texas A&M University, College Station, USA*
[2] *Institute for Nuclear Research, National Academy of Sciences of Ukraine, Kyiv, Ukraine*

*Corresponding author: sanjour@kinr.kiev.ua

ENERGY DENSITY FUNCTIONAL AND SENSITIVITY OF ENERGIES OF GIANT RESONANCES TO BULK NUCLEAR MATTER PROPERTIES

We provide a short review of the current status of the nuclear energy density functional (EDF) and the theoretical results obtained for properties of nuclei and nuclear matter. We will first describe a method for determining the parameters of the EDF, associated with the Skyrme type effective interaction, by carrying out a Hartree - Fock (HF)-based fit to the extensive set of data of ground-state properties and constraints. Next, we will describe the fully self-consistent HF-based random-phase-approximation (RPA) theory for calculating the strength functions $S(E)$ and centroid energies $E_{\rm CEN}$ of giant resonances and the folding model (FM) distorted wave Born approximation (DWBA) to calculate the excitation cross-section of giant resonances by α scattering. Then we will provide results for: (i) the Skyrme parameters of the KDE0v1 EDF; (ii) consequences of violation of self-consistency in HF-based RPA; (iii) FM-DWBA calculation of excitation cross-section; (iv) values of the $E_{\rm CEN}$ of isoscalar and isovector giant resonances of multipolarities $L=0-3$ for a wide range of spherical nuclei, using 33 EDFs associated with the standard form of the Skyrme type interactions, commonly employed in the literature; and (v) the sensitivities $E_{\rm CEN}$ of the giant resonances to bulk properties of nuclear matter (NM). We also determine constraints on NM properties, such as the incompressibility coefficient and effective mass, by comparing with experimental data on $E_{\rm CEN}$ of giant resonances.

Keywords: energy density functional, giant resonance, nuclear matter, strength function, random-phase-approximation.

1. Introduction

The atomic nucleus is a fascinating and important laboratory for the study of properties of a many-body system with strongly interacting constituents. Energy density functional (EDF) theory provides a powerful approach for theoretical calculations of properties of many-body systems. It is based on a theorem [1] for the existence of a universal EDF that depends on the densities of the constituents and their derivatives, which leads to the exact value for the ground state energy by minimization procedure. However, the main challenge is to find the EDF. An important task of the nuclear physics community is to develop a modern EDF which accounts for the effects of few-body and many-body correlations and provides enhanced predictive power for properties of nuclei and nuclear matter (NM), such as the NM incompressibility coefficient, $K_{\rm NM}$, and the density dependence of the symmetry energy, $E_{\rm sym}$, needed for determining the equation of states (EOS) of symmetric and asymmetric NM (ANM). It is well-known that knowledge of the NM equation of state is very important in the study of properties of nuclei, heavy-ion collisions and astrophysical phenomena [2, 3].

The phenomena of collective motions of strongly interacting nucleons in the many-body system of the atomic nucleus have been the subjects of experimental and theoretical investigations for many decades [4 – 7]. Of particular interest are the determination of properties of isoscalar (isospin $T=0$) and isovector ($T=1$) giant resonances of various multipolarities [8]. Over the years the strength function distributions, $S(E)$, and centroid energies, $E_{\rm CEN}$, of isoscalar and isovector giant resonances are sensitive to physical quantities of NM, such as the incompressibility coefficient $K_{\rm NM}$, and the effective mass m^*/m. The resulting constraints on the values of the bulk properties of NM can be used to determine the next generation EDF [9], with improved predictive power. We point out that in the following we present a short review of the current status of the nuclear EDF and the theoretical results obtained for properties of giant resonances in nuclei and of NM. For more extended reviews on the nuclear EDF and properties of giant resonances in nuclei and of NM, see Refs. [10 – 12] and references therein.

Since the earlier work of Brink and Vautherin [13], continuous efforts have been made to readjust the parameters of the Skyrme-type effective nucleon-nucleon (NN) interaction [14, 15] to improve the theoretical prediction of properties of nuclei [10, 16].

Many Skyrme type effective NN interactions of different forms were obtained by fitting the Hartree – Fock (HF) results to selected sets of experimental data [10, 16]. We emphasize that here we consider a specific standard form of the Skyrme type interaction, with ten (10) parameters [17]. We note that for fixed values for the nuclear matter properties the corresponding values for the Skyrme parameters can be determined by using the relations between the bulk properties of symmetric nuclear matter and the Skyrme parameters [9]. However, this is not possible due to the experimental uncertainties in the values of nuclear matter properties. It is common to determine the parameters of the Skyrme interaction by fitting experimental data on bulk properties of nuclei, such as binding energies and charge radii, and include the experimental data on nuclear matter properties as constraints. It is very important to note that in determining the parameters of the Skyrme interaction, various approximations, concerning: (i) the values of the neutron and proton masses; (ii) the spin-density terms may be ignored; (iii) the Coulomb exchange term is approximated or ignored; (iv) the center of mass correction to the energy is approximated. These approximations should be taken into account for a proper application of the specific interaction. In the following, we describe the method of determining the parameters of the very successful modern KDE0v1 Skyrme interaction [9] by a fit of the HF results to extensive experimental data of ground-state properties of the wide range of nuclei, excitation energies of the isoscalar giant monopole and including constraints such as the Landau stability conditions for nuclear matter.

In the next section we provide a short review of the formalism including: (i) the standard form of the Skyrme type interaction with ten (10) parameters and the corresponding EDF with the HF method for calculating ground state properties of nuclei; (ii) the RPA approach for calculating strength functions $S(E)$ and the centroid energies $E_{\rm CEN}$ of isoscalar and isovector giant resonances; (iii) the Folding-model (FM) distorted wave Born approximation (DWBA) for calculating excitation cross-section for giant resonances, and; (iv) the EOS of symmetric and ANM in terms of bulk properties of NM. In section 3 we present: (i) results of calculations of determination of the parameters of the standard Skyrme interaction; (ii) pointing out the consequences of carrying out fully self-consistent HF-based random-phase-approximation (RPA) calculations of $S(E)$ and $E_{\rm CEN}$ of giant resonances; (iii) pointing out the importance of carrying out microscopic calculations of excitation cross-sections of giant resonances; (iv) demonstrate the importance of carrying out a proper comparison between relativistic and non-relativistic calculations of $E_{\rm CEN}$, and; (v) present results of the calculated centroid energies, $E_{\rm CEN}$, of isoscalar $(T=0)$ and isovector $(T=1)$ giant resonances of multipolarity $L=0-3$ in ^{40,48}Ca, ^{68}Ni, ^{90}Zr, ^{116}Sn, ^{144}Sm, and ^{208}Pb nuclei, within fully self-consistent spherical HF-based RPA theory, using 33 effective NN Skyrme type interactions of the standard form. We also calculate the Pearson linear correlation coefficient to investigate the sensitivity of the $E_{\rm CEN}$ of each giant resonance of specific isospin and multipolarity to each bulk property of NM, such as the incompressibility coefficient, $K_{\rm NM}$, the effective mass m^*/m, the symmetry energy coefficients at ρ_0: $J=E_{\rm sym}[\rho_0]$, and its first and second derivatives L and $K_{\rm sym}$, respectively, and κ, the enhancement coefficient of the energy weighted sum rule (EWSR) of the isovector giant dipole resonance (IVGDR). By comparing to experimental data, we determined constraints on the properties of NM. In section 4, we present our summary and conclusions.

2. Formalism

2.1. Skyrme EDF

We adopt the following standard form for the Skyrme type effective NN interaction [17]:

$$V_{12}=t_0(1+x_0P_{12}^{\sigma})\delta(\mathrm{r}_1-\mathrm{r}_2)+\frac{1}{2}t_1(1+x_1P_{12}^{\sigma})[\overleftarrow{k}_{12}^2\,\delta(\mathrm{r}_1-\mathrm{r}_2)+\delta(\mathrm{r}_1-\mathrm{r}_2)\vec{k}_{12}^2]+$$

$$+t_2(1+x_2P_{12}^{\sigma})\overleftarrow{k}_{12}\delta(\mathrm{r}_1-\mathrm{r}_2)\vec{k}_{12}+\frac{1}{6}t_3(1+x_3P_{12}^{\sigma})\rho^{\alpha}\left(\frac{\vec{r}_1+\vec{r}_2}{2}\right)\delta(\mathrm{r}_1-\mathrm{r}_2)+$$

$$+iW_0\overleftarrow{k}_{12}\,\delta(\mathrm{r}_1-\mathrm{r}_2)(\sigma_1+\sigma_2)\cdot\vec{k}_{12}, \qquad (1)$$

where t_i, x_i, α, and W_0 are the ten (10) parameters of the interaction and P_{12}^{σ} is the spin-exchange operator, σ_i is the Pauli spin operator, $\vec{k}_{12}=-i\left(\vec{\nabla}_1-\vec{\nabla}_2\right)/2$, and $\overleftarrow{k}_{12}=-i\left(\overleftarrow{\nabla}_1-\overleftarrow{\nabla}_2\right)/2$. Here, the right and left arrows indicate that the momentum operators act on the right and the left, respectively. The Skyrme energy-density functional $H(r)$, associated with the interaction of Eq. (1), is given by [17],

$$H = K + H_0 + H_3 + H_{\text{eff}} + H_{\text{fin}} + H_{\text{so}} + H_{\text{sg}} + H_{\text{Coul}}\,, \tag{2}$$

where $K = \frac{\hbar^2}{2m}\tau$ is the kinetic-energy term. For the Skyrme interaction of Eq. (2), we have

$$H_0 = \frac{1}{4}t_0\left[(2+x_0)\rho^2 - (2x_0+1)\left(\rho_p^2+\rho_n^2\right)\right], \tag{3}$$

$$H_3 = \frac{1}{24}t_3\rho^{\alpha}\left[(2+x_3)\rho^2 - (2x_3+1)\left(\rho_p^2+\rho_n^2\right)\right], \tag{4}$$

$$H_{\text{eff}} = \frac{1}{8}\left[t_1(2+x_1)+t_2(2+x_2)\right]\tau\rho +$$

$$+\frac{1}{8}\left[t_2(2x_2+1)-t_1(2x_1+1)\right]\left(\tau_p\rho_p+\tau_n\rho_n\right), \tag{5}$$

$$H_{\text{fin}} = \frac{1}{32}\left[3t_1(2+x_1)-t_2(2+x_2)\right](\nabla\rho)^2 -$$

$$-\frac{1}{32}\left[3t_1(2x_1+1)+t_2(2x_2+1)\right]\left[(\nabla\rho_p)^2+(\nabla\rho_n)^2\right], \tag{6}$$

$$H_{\text{so}} = \frac{W_0}{2}\left[\mathrm{J}\cdot\nabla\rho + x_w\left(\mathrm{J}_p\cdot\nabla\rho_p + \mathrm{J}_n\cdot\nabla\rho_n\right)\right], \tag{7}$$

$$H_{\text{sg}} = -\frac{1}{16}(t_1x_1+t_2x_2)\mathrm{J}^2 + \frac{1}{16}(t_1-t_2)\left[\mathrm{J}_p^2+\mathrm{J}_n^2\right]. \tag{8}$$

Here, H_0 is the zero-range term, H_3 the density-dependent term, H_{eff} an effective-mass term, H_{fin} a finite-range term, H_{so} a spin-orbit term, H_{sg} is a term that is due to tensor coupling with spin and gradient and H_{Coul} is the contribution to the energy-density that is due to the Coulomb interaction. In Eqs. (3) – (8), $\rho = \rho_p + \rho_n$, $\tau = \tau_n + \tau_n$ and $\mathrm{J} = \mathrm{J}_n + \mathrm{J}_p$ are the particle number density, kinetic-energy density, and spin-density, respectively, with p and n denoting the protons and neutrons, respectively. Note that the additional parameter x_w, introduced in Eq. (7), allows us to modify the isospin dependence of the spin-orbit term. We have used the value of $\hbar^2/2m = 20.734$ MeV fm^2 in determining the parameters of the Skyrme interaction KDE0v1. We would like to emphasize that we have included the contributions from the spin-density term as given by Eq. (8), which is ignored in many Skyrme HF calculations. Although the contributions from the Eq. (8) to the binding energy and charge radii are not very significant, they are very crucial for the calculation of the Landau parameter G_0'. The corresponding mean-field V_{HF} and the total energy E of the system are given by

$$V_{\text{HF}} = \frac{\delta H}{\delta\rho}, \quad E = \int H(\mathrm{r})\,d\mathrm{r}\,, \tag{9}$$

where, the Skyrme energy-density functional $H(r)$, is given in Eq. (2).

In a spherical nucleus, the single-particle wave function can be written as a product of the radial function $R_n(r)$, the spherical harmonic function $Y_{jlm}(\mathrm{r},\sigma)$, and the isospin function $\chi_{m_\tau}(\tau)$,

$$\phi_n(\mathrm{r},\sigma,\tau) = \frac{R_n(r)}{r}Y_{jlm}(\mathrm{r},\sigma)\chi_{m_\tau}(\tau)\,. \tag{10}$$

Assuming a closed-shell spherical nucleus, we use Eq. (10) to achieve the final form of the HF equations for spherical coordinates:

$$\frac{\hbar^2}{2m_\tau^*(r)}\left[-R_n''(r)+\frac{l_n(l_n+1)}{r^2}R_n(r)\right] - \frac{d}{dr}\left(\frac{\hbar^2}{2m_\tau^*(r)}\right)R_n'(r) +$$

$$+\left[U_\tau(r)+\frac{1}{r}\frac{d}{dr}\left(\frac{\hbar^2}{2m_\tau^*(r)}\right)+\frac{\left[j_n(j_n+1)-l_n(l_n+1)-\frac{3}{4}\right]}{r}W_\tau(r)\right]R_n(r) = \varepsilon_n R_n(r)\,. \tag{11}$$

where $m_\tau^*(r)$, $U_\tau(r)$ and $W_\tau(r)$ are the effective mass, the single-particle potential, and the spin-orbit potential, respectively. They are given in terms of the Skyrme parameters and the nuclear densities. An initial guess is taken for the single-particle wave functions such as WS wave functions. The HF equations are then solved by iteration.

2.2. Self-consistent HF-based RPA

The response function $S(E)$ of the many-body system to an external field described by the single-particle operator, $F = \sum f(r_i)$, is given by [18]

$$S(E)=\sum_{\nu}\left|\langle 0|F|\nu\rangle\right|^2\delta(E-E_{\nu})=$$

$$=\frac{1}{\pi}\mathrm{Im}\int_0^{\infty}dr\,dr'\,f(r)G(r,r',E)\,f(r'), \qquad (12)$$

where G is the particle-hole Green function and the sum is over all RPA states ν of energy E_{ν}. The transition density ρ_t associated with the strength in the region $E\pm\Delta E$ is obtained from:

$$\rho_t(r,E)=\frac{\Delta E}{\sqrt{S(E)\Delta E}}\int_0^{\infty}f(r')\left[\frac{1}{\pi}\mathrm{Im}\,G(r',r,E)\right]dr'. \qquad (13)$$

The RPA Green function is given by

$$G^{\mathrm{RPA}}=G^{(0)}\left(1-\frac{\delta V}{\delta\rho}G^{(0)}\right)^{-1}. \qquad (14)$$

Here, V is the HF potential, having a functional dependence on ρ, the density. The unperturbed Green function $G^{(0)}$ is given in terms of the HF Hamiltonian H, its occupied eigenstates ϕ_h, and the corresponding eigenenergies ε_h, as

$$G^{(0)}(r_1,r_2,\omega)=-\sum_h\phi_h(r_1)\times$$

$$\times\left(\frac{1}{H-\varepsilon_h-\omega}+\frac{1}{H-\varepsilon_h+\omega}\right)\phi_h(r_2). \qquad (15)$$

The sum in (15) is on the occupied states; $(H-E)^{-1}$ is the HF Green function for a single particle propagated from r_2 to r_1.

The electromagnetic single-particle scattering operator for the isoscalar $(T=0)$ excitation of multipolarity L is given by [19],

$$F_L=\sum_i f(r_i)Y_{L0}(i), \qquad (16)$$

and the corresponding isovector ($T=1$) single-particle scattering operator is given by,

$$F_L=\frac{Z}{A}\sum_n f(r_n)Y_{L0}(n)-\frac{N}{A}\sum_p f(r_p)Y_{L0}(p). \qquad (17)$$

The $S(E)$ of the different multipolarities is then determined by: $f(r)=r^2$, for the isoscalar and isovector monopole $(L=0)$ and quadrupole $(L=2)$, $f(r)=r^3$ for the octupole $(L=3)$, $f(r)=r$ for the isovector dipole $(T=1,\ L=1)$, and lastly $f(r)=r^3-(5/3)\langle r^2\rangle r$ for the isoscalar dipole $(T=0,\ L=1)$. We point out that for the isoscalar dipole we subtract the contribution from the spurious state [20, 21]. We calculate the energy moments of the $S(E)$ using

$$m_k=\int_{E_1}^{E_2}E^kS(E)\,dE, \qquad (18)$$

where E_2-E_1 is the appropriate experimental excitation energy range. The centroid energies of the resonances are then obtained using:

$$E_{\mathrm{CEN}}=m_1/m_0. \qquad (19)$$

For $E_1=0$ and $E_2=\infty$, the first energy moment, m_1, of the isoscalar operator F_L may also be directly obtained from the HF ground state wave function:

$$m_1(L,T=0)=\frac{1}{4\pi}\frac{\hbar^2}{2m}\int_0^{\infty}g_L(r)\rho(r)4\pi r^2dr, \qquad (20)$$

thus, leading to the EWSR [4]. In Eq. (20) $\rho(r)$ is the ground state density obtained from the HF ground state of the nucleus, while $g_L(r)$ depends on the multipolarity, L, and its $f(r)$:

$$g_L(r)=\left(\frac{df}{dr}\right)^2+L(L+1)\left(\frac{f}{r}\right)^2. \qquad (21)$$

The isovector EWSR is related to Eq. (20) by:

$$m_1(L,T=1)=\frac{NZ}{A^2}m_1(L,T=0)[1+\kappa-\kappa_{np}], \qquad (22)$$

where κ is an enhancement coefficient which is due to the momentum dependence of the effective NN interaction, given for the standard Skyrme-type interaction Eq. (1) by:

$$\kappa=\frac{(1/2)[t_1(1+x_1/2)+t_2(1+x_2/2)]}{(\hbar^2/2m)(4NZ/A^2)}\times$$

$$\times\frac{2\int g_L(r)\rho_p(r)\rho_n(r)4\pi r^2dr}{\int g_L(r)\rho(r)4\pi r^2dr}, \qquad (23)$$

while the correction factor κ_{np} arises from the small differences between the neutron and proton densities, or in other words because $\rho_n(r)-\rho_p(r)\neq\frac{N-Z}{A}\rho(r)$, and is obtained from:

$$\kappa_{np}=\frac{(N-Z)}{A}\frac{A}{NZ}\frac{\int g_L(r)[Z\rho_n(r)-N\rho_p(r)]4\pi r^2dr}{\int g_L(r)\rho(r)4\pi r^2dr}. \qquad (24)$$

We note that here we adopt the methods of Refs. [18, 19, 22] in the numerical evaluation of the strength functions and centroid energies of the giant resonances.

2.3. DWBA calculations of excitation cross-section

The distorted wave Born approximation (DWBA) has been employed successfully for the theoretical description of low-energy scattering reactions [23, 24]. The DWBA differential cross-section for the excitation of a nucleus by inelastic scattering by alpha (α) particle, $\alpha + \mathrm{N} \to \alpha + \mathrm{N}^*$, is given by

$$\frac{d\sigma^{\mathrm{DWBA}}}{d\Omega} = \left(\frac{\mu}{2\pi\hbar^2}\right)^2 \frac{k_\mathrm{f}}{k_\mathrm{i}} |T_\mathrm{fi}|^2, \qquad (25)$$

where k_i and k_f are the initial and final linear momenta of the α-nucleus relative motion, respectively, and μ is the reduced mass. The transition matrix element T_fi is given by

$$T_\mathrm{fi} = \left\langle \chi_\mathrm{f}^{(-)} \Psi_\mathrm{f} \middle| V \middle| \chi_\mathrm{i}^{(+)} \Psi_\mathrm{i} \right\rangle , \qquad (26)$$

where V is the α-nucleon interaction, $\chi_\mathrm{i}^{(+)}$ and $\chi_\mathrm{f}^{(-)}$ are the incoming and outgoing distorted wave functions of the relative α-nucleus motion, respectively, Ψ_i and Ψ_f are the initial and final states of the nucleus, respectively. To calculate the transition matrix element T_fi, Eq. (26), one can adopt the following approach. First, integrate over the coordinates of the nucleons (in Ψ_i and Ψ_f) to obtain the transition potential

$$\delta U(\mathrm{r}) \sim \int \Psi_\mathrm{f}^* V \Psi_\mathrm{i} \, d\mathrm{r}_1 d\mathrm{r}_2 \ldots d\mathrm{r}_A \qquad (27)$$

as a function of the relative coordinate r between the projectile and the nucleus and then calculate the cross-section using

$$\frac{d\sigma}{d\Omega} = \left(\frac{\mu}{2\pi\hbar^2}\right)^2 \frac{k_\mathrm{f}}{k_\mathrm{i}} \left| \left\langle \chi_\mathrm{f}^{(-)} \middle| \delta U \middle| \chi_\mathrm{i}^{(+)} \right\rangle \right|^2 . \qquad (28)$$

The cross-section is calculated using a certain DWBA code [25] with the transition potential $\delta U(r)$ and the optical potential $U(r)$ as input.

The folding model (FM) approach [23] to determine the optical potential $U(r)$ and transition potential $\delta U(r)$, as convolutions between the projectile-nucleon interaction $V(|\mathrm{r}-\mathrm{r}'|, \rho_0(r'))$ and the ground state and transition densities, respectively, is commonly used in theoretical descriptions of α-particle scattering [24]. The optical potential $U(r)$ is given by

$$U(r) = \int d\mathrm{r}' V(|\mathrm{r}-\mathrm{r}'|, \rho_0(r')) \rho_0(r'). \qquad (29)$$

Here, $\rho_0(r')$ is the ground state HF density of a spherical target nucleus and the α-nucleon interaction $V(|\mathrm{r}-\mathrm{r}'|, \rho_0(r'))$ is assumed to have the parameterized form

$$V(|\mathrm{r}-\mathrm{r}'|, \rho_0(r')) = -V_0 \left(1 + \beta_V \rho_0^{2/3}(r')\right) e^{\frac{-|\mathrm{r}-\mathrm{r}'|}{\alpha_V}} -$$

$$- iW_0 \left(1 + \beta_W \rho_0^{2/3}(r')\right) e^{\frac{-|\mathrm{r}-\mathrm{r}'|}{\alpha_W}} . \qquad (30)$$

Note that $V(|\mathrm{r}-\mathrm{r}'|, \rho_0(r'))$ is complex and density-dependent [24]. The parameters V_0, β_V, α_V, W_0, β_W, α_W in Eq. (30) are usually determined by a fit to the elastic scattering data. The transition potential, $\delta U_L(r,E)$, for an excited state with the multipolarity L and excitation energy E, is obtained from

$$\delta U_L(r,E) = \int d\mathrm{r}' \delta\rho_L(\mathrm{r}',E) \left[V(|\mathrm{r}-\mathrm{r}'|, \rho_0(r')) + \rho_0(r') \frac{\partial V(|\mathrm{r}-\mathrm{r}'|, \rho_0(r'))}{\partial \rho_0(r')} \right], \qquad (31)$$

where $\delta\rho_L(\mathrm{r}',E)$ is the transition density for the excited state. We point out that within the "macroscopic" approach, commonly employed in the experimental analysis of scattering data, one adopts semiclassical collective model transition densities, ρ_{coll}, [21, 23, 24, 26, 27] with radial forms that are independent of the excitation energy and are derived from the ground state density using a collective model.

Another approach for evaluating the transition matrix element T_fi, usually employed in theoretical calculations, is to first integrate over the relative α-nucleus coordinates to obtain the scattering operator,

$$O \sim \int \chi_\mathrm{f}^{(-)*} V \chi_\mathrm{i}^{(+)} \, d\mathrm{r} , \qquad (32)$$

and then calculate the matrix element $\left\langle \Psi_\mathrm{f} \middle| O \middle| \Psi_\mathrm{i} \right\rangle$ within a theoretical model for Ψ_i and Ψ_f, using the HF ground state density in (29) and the HF-based RPA transition density in (31). Note that it is quite common in theoretical calculations to adopt for the operator O in (32) the operators of Eqs. (16) and (17), for determining the strength function $S(E)$. Therefore, for a proper comparison between experimental and theoretical results for $S(E)$, one should adopt the

"microscopic" FM approach in the DWBA calculations of $\sigma(E)$, using HF ground state density in (29) and the HF-based RPA transition density in (31).

2.4. Equation of state of symmetric and asymmetric nuclear matter

In the vicinity of the saturation density ρ_0 of symmetric NM, the EOS can be approximated by

$$E_0[\rho] = E_0[\rho_0] + \frac{1}{18} K_{\rm NM} \left(\frac{\rho - \rho_0}{\rho_0} \right)^2, \qquad (33)$$

where $E_0[\rho]$ is the binding energy per nucleon and $K_{\rm NM}$ is the incompressibility coefficient which is proportional to the curvature of the EOS, $K_{\rm NM} = 9\rho_0^2 \frac{\partial^2 E_0}{\partial \rho^2}\Big|_{\rho_0}$. The EOS of asymmetric NM (ANM) can be approximated by

$$E[\rho_n, \rho_p] = E_0[\rho] + E_{\rm sym}[\rho] \left(\frac{\rho_n - \rho_p}{\rho} \right)^2, \qquad (34)$$

where ρ_p is the proton density, ρ_n is the neutron density and $E_{\rm sym}[\rho]$ is the symmetry energy at matter density ρ, given by

$$E_{\rm sym}[\rho] = J + \frac{1}{3} L \left(\frac{\rho - \rho_0}{\rho_0} \right) + \frac{1}{18} K_{\rm sym} \left(\frac{\rho - \rho_0}{\rho_0} \right)^2, \qquad (35)$$

where $J = E_{\rm sym}[\rho_0]$ is the symmetry energy at saturation density ρ_0, $L = 3\rho_0 \frac{\partial E_{\rm sym}}{\partial \rho}\Big|_{\rho_0}$, and $K_{\rm sym} = 9\rho_0^2 \frac{\partial^2 E_{\rm sym}}{\partial \rho^2}\Big|_{\rho_0}$. Therefore, to extend our knowledge of the EOS, accurate values of $K_{\rm NM}$, $E_{\rm sym}[\rho_0]$ and its first and second derivatives are needed in the vicinity of the symmetric NM saturation density. Here we consider the sensitivity of the centroid energies of the isoscalar and isovector giant resonances to bulk properties of NM, such as $K_{\rm NM}$, $E_{\rm sym}$ and the effective mass m^*/m.

3. Results

3.1. Determination of the parameters of the Skyrme interaction

Many Skyrme type effective NN interactions of different forms were obtained during the last five decades by fitting the HF results to selected sets of experimental data [9, 10]. We emphasize that here we consider the specific standard form of Eq. (1) for the Skyrme type interaction. We note that for a fixed set of values for the bulk properties of NM the corresponding values for the Skyrme parameters can be determined by using the relations between the properties of nuclear matter and the Skyrme parameters [9, 17]. However, this is not possible due to the large uncertainties in the experimental values of the bulk properties of NM. It is common to determine the parameters of the Skyrme interaction by fitting HF results to experimental data on properties of nuclei, such as binding energies and charge radii, and include the experimental data on bulk properties of NM as constraints. For example, in the case of the modern KDE0v1 Skyrme interaction [9] the parameters were determined by a fit of the HF results to experimental data for binding energies and charge radii of an extended set of ground states of nuclei, which include neutron-rich as well as proton-rich nuclei. The experimental data for the spin-orbit (S-O) splitting of the $2p$ neutrons and protons "bare" single-particle orbits in the ^{56}Ni nucleus and the rms radii for the $1d_{5/2}$, $r_{\rm v}(\nu 1d_{5/2})$, and $1f_{7/2}$, $r_{\rm v}(\nu 1f_{7/2})$, neutron orbits in ^{17}O and ^{41}Ca nuclei, respectively, were also included in the fit. We note, in particular, that the experimental data for the isoscalar giant monopole resonance (ISGMR) constraint energies E_0 for the ^{90}Zr, ^{116}Sn, ^{144}Sm, and ^{208}Pb nuclei and the critical density $\rho_{\rm cr}$, determined by imposing the Landau stability [28] conditions for nuclear matter, up to the value of $2.5\rho_0$ with an error of $0.5\rho_0$, where ρ_0 is the saturation density, were also included in the fit. Moreover, the values of the Skyrme parameters were constrained by the experimental data on the bulk properties of NM and by requiring that: (i) a positive slope for the symmetry energy density for $\rho < 3\rho_0$; (ii) value of $\kappa = 0.1 - 0.5$ for the enhancement factor of the EWSR for the IVGDR and (iii) value of $G_0' > 0$ for the Landau particle-hole interaction parameter at $\rho = \rho_0$. The simulated annealing approach was employed in the minimization procedure to determine the Skyrme parameters with the best fit to the experimental data (see Ref. [9]).

It is very important to note that in determining the parameters of the Skyrme interaction, various approximations were made in the literature concerning: (i) the values of the neutron and proton masses; (ii) the spin-density terms may be ignored; (iii) the Coulomb exchange term is approximated or ignored; (iv) the center of mass correction to the energy is approximated; (v) the contribution of charge dependence terms in the NN interaction is usually neglected.

These approximations should be taken into account for a proper application of the specific interaction. In Table 1 we present three parameter sets: for the SkM* force [29], which gives the realistic values of the nuclear matter incompressibility and the deformation energies of heavy nuclei, for the more recent Sly4 interaction [17] and the most recent KDE0v1 interaction [9]. We point out that knowledge of the surface energy of finite nuclei provides an additional relation involving Skyrme parameters t_1 and t_2. We note that in the mean-field, adjusted to reproduce the experimental data of charge root-mean-square (RMS) radii, the calculated Coulomb displacement energies of analog states are smaller than the experimental data by about 7 % [30]. It was shown [30 – 33] that this discrepancy is due to the neglect of the contributions of charge dependence in the nuclear force and the effect of long-range correlations. A good approximation for accounting for these contributions and also obtaining a good fit for binding energies of proton-rich nuclei is to eliminate the contribution of the exchange coulomb term from the Hamiltonian, i.e. taking $C_{\text{ex}} = 0$, as was done in determining the parameters of the KDE0v1 Skyrme interaction [9], see Table 1. We note that the Skyrme interaction KDE0v1 also reproduces the experimental data of neutron stars and fission barriers [16], which were not included in the fit for determining the parameters of KDE0v1.

Table 1. **Parameters of the Skyrme interactions SKM* [29], Sly4 [17], and KDE0v1 [9] and some associated properties of symmetric nuclear matter. The values of C_{ex} = 0 or 1 indicate whether the Coulomb exchange term is omitted or included in the Hamiltonian**

Force	SkM*	Sly4	KDE0v1
t_0, MeV fm^3	–2645.0	–2488.91	–2553.0843
t_1, MeV fm^5	410.0	486.82	411.6963
t_2, MeV fm^5	–135.0	–546.39	–419.8712
t_3, MeV fm$^{3(1+\alpha)}$	15595.0	13777.0	14603.6069
x_0	0.09	0.834	0.6483
x_1	0.0	–0.344	–0.3472
x_2	0.0	–1.0	–0.9268
x_3	0.0	1.354	0.9475
α	1/6	1/6	0.1673
W_0, MeV fm^5	130.0	123.0	124.4100
C_{ex}	1	1	0
$E_0[\rho_0]$, MeV	–15.78	–15.97	–16.23
K_{NM}	216.7	229.90	227.54
ρ_0, fm^{-3}	0.16	0.16	0.165
m^*/m	0.79	0.70	0.74
J, MeV	30.03	32.00	34.58
L, MeV	45.78	45.96	54.69
κ	0.53	0.25	0.23

3.2. Consequences of violations of self-consistency in RPA calculation

Accurate experimental data on the strength distributions, energies, and widths of various giant resonances exist for a wide range of nuclei [6, 34]. At present, the results of our fully self-consistent and HF-based RPA calculations for centroid energies of various giant resonances are accurate within 0.1 - 0.2 MeV, comparable to the current experimental accuracy [34]. In the following, we will describe and present results of the investigations leading to the resolutions of the longstanding discrepancy in the value of K_{NM}, as deduced using Skyrme interactions ($K_{\text{NM}} = 210$ MeV) and Gogny interaction ($K_{\text{NM}} = 230$ MeV).

Violation of self-consistency in the HF-based RPA calculations of properties of giant resonances, such as the response functions $S(E)$ and centroid energies E_{CEN}, are mainly due to the neglect of some components of the NN interaction, such as the Coulomb and spin-orbit interactions, which were included in the HF calculations but not in the RPA calculations and to the limitation in the configuration space (i.e. numerical accuracy). We point out that the fulfillment of the EWSR of the giant resonances and obtaining the $L = 1, T = 0$ spurious state, associated with the center of mass motion, at zero energy are necessary conditions for self-consistency in the HF-based RPA calculations, but not sufficient. The effects of violations of self-consistency in HF-based RPA calculations of $S(E)$, E_{CEN} and the transition densities ρ_t of various giant resonances were investigated in detail [19 – 21, 35]. Violations of self-consistency may have significant effects on the $S(E)$, E_{CEN} and ρ_t of the ISGMR and on the ISGDR [19, 20].

The HF-based RPA results of the strength functions $S(E)$ of the ISGMR in ^{208}Pb and ^{90}Zr, obtained using the KDE0 Skyrme interaction [9], are shown in Fig. 1. The full line (SC) corresponds to the fully self-consistent calculations. The dashed line and the open circle line represent the results for $S(E)$ obtained by neglecting the spin-orbit and Coulomb particle-hole interactions in the RPA calculations, respectively. The results of similar calculations for isoscalar giant resonances of multipolarity $L = 0 - 3$, using the SGII Skyrme interaction [36], are shown in Fig. 2 for ^{100}Sn. We point out the violations of self-consistency result in a reduction of about 1 MeV (of about a 7 %) in the ISGMR energy of ^{208}Pb. This shift leads to about a 14 % decrease in the value of the nuclear matter incompressibility coefficient K_{NM}, which corresponds to a shift of 30 MeV in K_{NM}. Therefore, we conclude that when compared

with experimental data, the same value of K_{NM} is obtained for different non-relativistic interactions, such as Skyrme and Gogny interactions, if the HF-based RPA calculations of the centroid energy of the ISGMR are fully self-consistent. As shown in Fig. 2, the effects of violations of self-consistency on E_{CEN} of isoscalar giant resonances of multipolarity $L=1-3$ are relatively small. A similar, relatively small shift in the values of the E_{CEN} of isovector giant resonances was obtained, see Ref. [19].

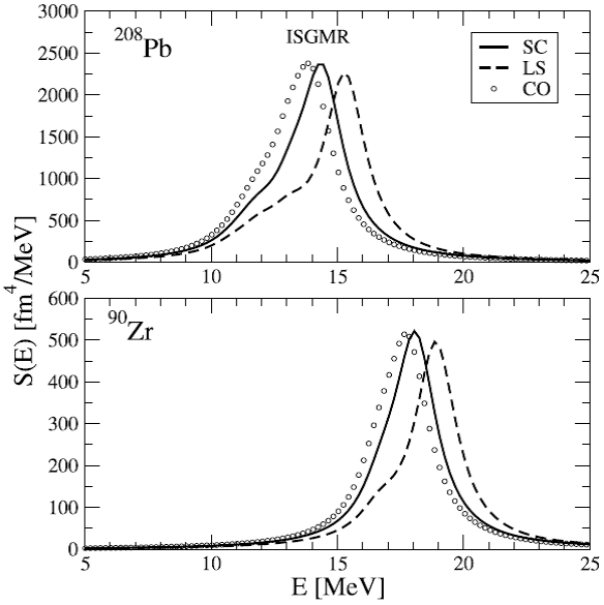

Fig. 1. Strength functions of isoscalar giant monopole for ^{208}Pb and ^{90}Zr nuclei calculated using the KDE0 interaction [9]. SC (full line) corresponds to the fully self-consistent calculation where LS (dashed line) and CO (open circle) represent the calculations without the particle-hole spin-orbit and Coulomb interactions in the RPA calculations, respectively.

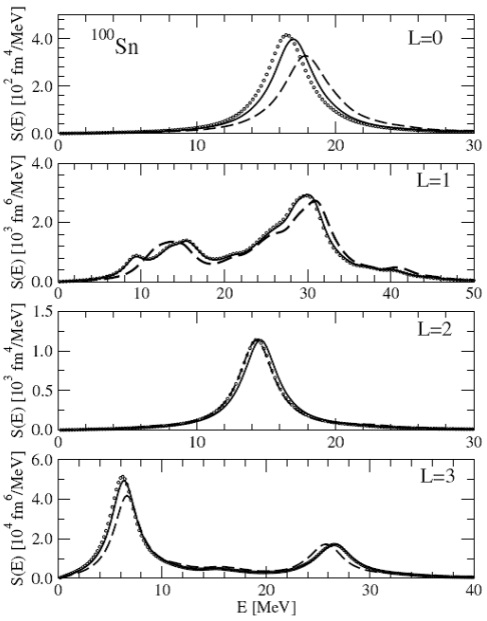

Fig. 2. HF-RPA results for the isoscalar strength functions of ^{100}Sn for multipolarities $L=0-3$ are displayed. SC (full line) corresponds to fully self-consistent calculations where LS (dashed line) and CO (open-circle) represent the calculations without the particle-hole spin-orbit and Coulomb interactions in the RPA calculations, respectively. The Skyrme interaction SGII [36] was used (Taken from Ref. [19]).

3.3. Nuclear matter incompressibility coefficient from the ISGDR

The isoscalar giant dipole resonance (ISGDR) is a compression mode and provides an independent source of information on the NM incompressibility coefficient K_{NM}. Early experimental investigations [37] resulted in a value of about 20 MeV for the E_{CEN} of the ISGDR in ^{208}Pb, which is smaller by about 4 MeV than the prediction of fully self-consistent HF-based RPA results obtained with interactions adjusted to reproduce experimental values of the E_{CEN} for ISGMR in ^{208}Pb. Therefore, the early experimental data on the E_{CEN} of ISGDR leads to a significantly smaller value of K_{NM} ($\sim$170 MeV) than that obtained from the ISGMR, which raises some doubts concerning the unambiguous extraction of K_{NM} from energies of compression modes of nuclei. To investigate this discrepancy, we have therefore carried out microscopic calculation of the excitation cross-section of the ISGDR, within the FM DWBA using the HF ground state matter density and the RPA transition density, see section 2.3.

In Fig. 3 we present the results [21] of microscopic calculations of the excitation cross-section $\sigma(E)$ of the ISGDR in ^{116}Sn by 240 MeV α-particle scattering, carried out within the microscopic HF-based RPA and the FM-DWBA theory [23, 24] using the SL1 Skyrme interaction [38]. The solid line in the upper panel shows the HF-based RPA results for the fraction of the EWSR, $ES(E)/\mathrm{EWSR}$. The middle panel of the figure shows the double differential ISGDR cross-sections at the angle of 1st maximum found using the transition potential for the ISGDR obtained from the HF-based RPA transition density. The lowest panel shows the results of the second panel (solid line) and from the collective model transition density ρ_{coll} [39] (dashed line) both normalized to 100 % of the EWSR of the ISGDR. Now, considering the solid line values of the cross-section shown in the middle panel as the "experimental data" and dividing it by the cross-section values shown by the dashed line (semi-classical results) in the lower panel, we obtain the values of $ES(E)/\mathrm{EWSR}$ shown by the dashed line in the upper panel, which is the result

obtained in the experimental analysis of cross-section data using the semi-classical form for the energy-independent transition density.

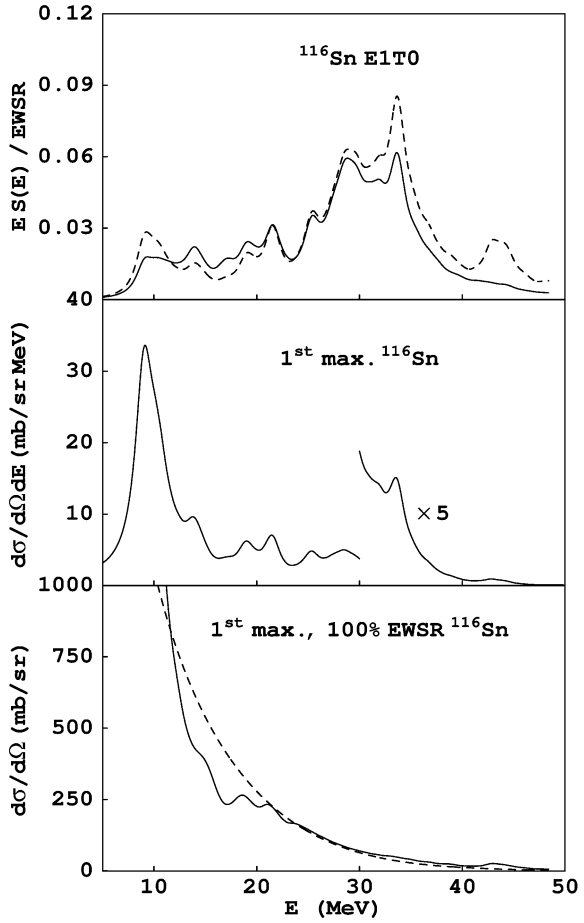

Fig. 3. Reconstruction of the ISGDR EWSR in ^{116}Sn from the inelastic α-particle cross-sections. The middle panel: 1st maximum double differential cross-section obtained from the RPA transition density ρ_t. The lower panel: maximum cross-section obtained with the collective model transition density ρ_{coll} (dashed line) and the HF-RPA transition density ρ_t (solid line) normalized to 100 % of the EWSR. Upper panel: the solid (dashed) line is the ratio between the middle panel curve and the solid (dashed) curve of the lower panel (Taken from Ref. [21]).

It is seen from the upper panel that using of the collective model transition densities ρ_{coll} in analyzing the experimental cross sections increases the EWSR by about 15 %. However, the shifts in the centroid energies are small (a few percents), similar in magnitude to the current experimental uncertainties. It is important to note [21] that the maximum cross-section for the excitation of the ISGDR shown in the middle panel decreases strongly at high excitation energy and drops below the experimental sensitivity. This missing experimental strength leads to a reduction of about 3.0 MeV in the centroid energy of the ISGDR. Taking into account this missing strength significantly reduces the discrepancy between theory and experiment. This prediction was confirmed in an improved experiment [40]. Therefore, we conclude that the value of K_{NM} deduced from the ISGDR compression mode is in good agreement with that deduced from the ISGMR compression mode.

3.4. Incompressibility coefficient of NM in relativistic and nonrelativistic models

Some relativistic RPA models yielded values of K_{NM}, deduced from the ISGMR, which are significantly larger than those obtained from the non-relativistic Skyrme HF-based RPA calculations. For example, the NL3 parameterization [41] is associated with $K_{NM} = 272$ MeV, as compared to the value of $K_{NM} = 240$ MeV deduced from the non-relativistic model. We have investigated this model's dependence in Ref. [42] by generating parameter sets for Skyrme interactions by the least square fitting procedure using the same experimental data for the bulk properties of nuclei considered in Ref. [41] for determining the NL3 parameterization of the effective Lagrangian used in the relativistic mean-field (RMF) models. It is important to point out that the symmetry energy coefficient J and charge rms radius of ^{208}Pb were constrained to be very close to 37.4 MeV and 5.50 fm, respectively, as obtained with the NL3 interaction and K_{NM} was fixed in the vicinity of the NL3 value $K_{NM} = 271.76$ MeV.

Table 2 presents the results for E_{CEN} of the ISGMR for several nuclei, obtained within fully self-consistent HF-based RPA (see Ref. [35]), using the KDE0 [9], SK255 [42], and SGII [36] Skyrme interactions, and the results obtained within the relativistic mean-field (RMF)-based RPA using the NL3 interaction [41]. We also compare with the experimental data of Refs. [40, 43] calculated using the experimental excitation energy range $(\omega_1 - \omega_2)$. We point out that the results of Table 2 demonstrate that K_{NM} can be deduced in a model-independent way using relativistic and non-relativistic RPA calculations. Therefore, we conclude that $K_{NM} = 240 \pm 20$ MeV. The uncertainty of 20 MeV is mainly due to the uncertainty in $E_{sym}[\rho]$ and the possible effects of correlations beyond mean-field-based RPA. Note the difference in the value of J associated with SGII and the SK255 Skyrme interactions, and with the NL3 interaction shown in Table 2.

Table 2. **Results of fully self-consistent RPA calculations for the centroid energies of the ISGMR for interactions with various values of K_{NM} and J coefficients (in MeV)**

Nucleus	$\omega_1 - \omega_2$	Experiment	NL3	SK255	SGII	KDE0
^{90}Zr	0 - 60		18.7	18.90	17.89	18.03
	10 - 35	17.81 ± 0.30		18.85	17.87	17.98
^{116}Sn	0 - 60		17.1	17.31	16.36	16.58
	10 - 35	15.85 ± 0.20		17.33	16.38	16.61
^{144}Sm	0 - 60		16.1	16.21	15.26	15.46
	10 - 35	15.40 ± 0.40		16.19	15.22	15.44
^{208}Pb	0 - 60		14.2	14.34	13.57	13.79
	10 - 35	13.96 ± 0.20		14.38	13.58	13.84
$K_{\rm NM}$, MeV			272	255	215	229
J, MeV			37.4	37.4	26.8	33.0

3.5. The sensitivity of energies of giant resonances to properties of nuclear matter

The sensitivities of the strength function distributions, $S(E)$, and centroid energies, $E_{\rm CEN}$, of isoscalar and isovector giant resonances of nuclei to the values of bulk properties of symmetric $(N = Z)$ NM: such as the binding energy per nucleon $E_0[\rho_0]$, the saturation density ρ_0, the incompressibility coefficient $K_{\rm NM} = 9\rho_0^2 \left.\frac{\partial^2 E_0}{\partial \rho^2}\right|_{\rho_0}$, the symmetry energy coefficients at ρ_0, $J = E_{\rm sym}[\rho_0]$, and its first and second derivatives $L = 3\rho_0 \left.\frac{\partial E_{\rm sym}}{\partial \rho}\right|_{\rho_0}$ and $K_{\rm sym} = 9\rho_0^2 \left.\frac{\partial^2 E_{\rm sym}}{\partial \rho^2}\right|_{\rho_0}$, respectively, the effective mass m^*/m, and the enhancement coefficient κ of the EWSR of the IVGDR, have been investigated extensively very recently [8]. In this investigation:

1. The isoscalar and isovector giant resonances of multipolarities $L = 0$ to 3 were considered for the wide range of closed-shell nuclei ^{40,48}Ca, ^{68}Ni, ^{90}Zr, ^{116}Sn, ^{144}Sm, and ^{208}Pb. The occupation number approximation for the single-particle orbits for the open-shell nucleus ^{144}Sm was adopted to ensure a spherical nucleus.

2. Fully self-consistent HF-based RPA calculations of the centroid energies were carried out using 33 Skyrme effective NN interactions of the standard form, Eq. (1), commonly adopted in the literature. The interactions used in this work are: SGII [36], KDE0 [9], KDE0v1 [9], SKM* [29], SK255 [42], SkI3 [44], SkI4 [44], SkI5 [44], SV-bas [45], SV-min [45], SV-sym32 [45], SV-m56-O [46], SV-m64-O [46], Sly4 [17], Sly5 [17], Sly6 [17], SkMP [47], SkO [48], SkO′ [48], LNS [49], MSL0 [50], NRAPR [51], SQMC650 [52], SQMC700 [52], SkT1 [53], SkT2 [53], SkT3 [53], SkT8 [53], SkT9 [53], SkT1* [53], SkT3* [53], Skxs20 [54] and Zσ [55]. We note that wide ranges of values for the bulk NM properties are covered by the selected Skyrme interactions [8].

3. The Skyrme interactions were implemented in these calculations as they were designed. For example, by using the values of the masses of the proton and the neutron and the approximation for the Coulomb energy that were adopted in determining the parameters of the interactions. Self-consistency was ensured by including in the RPA calculations all the components of the interaction used in the HF calculation and carrying out highly accurate numerical calculations.

4. The sensitivity of $E_{\rm CEN}$ to a NM property was deduced by calculating the corresponding Pearson linear correlation coefficient C, given, for quantities x and y, by

$$C = \frac{\sum_{i=1}^{n}(x_i - \bar{x})(y_i - \bar{y})}{\sqrt{\sum_{i=1}^{n}(x_i - \bar{x})^2}\sqrt{\sum_{i=1}^{n}(y_i - \bar{y})^2}}, \qquad (36)$$

where $\bar{x}$ and $\bar{y}$ are the averages of x and y and the sum runs over all values. The different degrees of correlation can be classified as: strong $(|C| > 0.80)$, medium $(|C| = 0.61 - 0.80)$, weak $(|C| = 0.35 - 0.60)$ and no correlation $(|C| < 0.35)$.

In Table 3 the calculated Pearson linear correlation coefficients between different sets of NM properties are shown. We point out the weak correlation between $K_{\rm NM}$ and m^*/m, the medium correlation between m^*/m and the enhancement coefficient for the EWSR of the IVGDR, κ, and the varying degrees of correlation between the symmetry energy coefficients J, L and $K_{\rm sym}$.

Table 3. **Calculated Pearson linear correlation coefficients, *C*, for NM properties. The parameters of all 33 Skyrme effective NN interactions were used to calculate *C* (see Ref. [8])**

	$K_{\rm NM}$	J	L	$K_{\rm sym}$	m^*/m	κ	$W_0\ (x_w=1)$
$K_{\rm NM}$	1.00	0.03	0.30	0.43	–0.37	–0.02	0.03
J	0.03	1.00	0.72	0.49	0.07	–0.24	–0.25
L	0.30	0.72	1.00	0.91	–0.15	–0.13	–0.08
$K_{\rm sym}$	0.43	0.49	0.91	1.00	–0.41	–0.08	0.05
m^*/m	–0.37	0.07	–0.15	–0.41	1.00	–0.63	–0.19
κ	–0.02	–0.24	–0.13	–0.08	–0.63	1.00	–0.03
$W_0\ (x_w=1)$	0.03	–0.25	–0.08	0.05	–0.19	–0.03	1.00

Table 4 presents the Pearson linear correlation coefficients between each nuclear bulk property of nuclear matter at saturation density and centroid energy of each giant resonance: the isoscalar giant monopole resonance (ISGMR), isoscalar giant dipole resonance (ISGDR), isoscalar giant quadrupole resonance (ISGQR), isoscalar giant octupole resonance (ISGOR), isovector giant monopole resonance (IVGMR), isovector giant dipole resonance (IVGDR), isovector giant quadrupole resonance (IVGQR) and isovector giant octupole resonance (IVGOR). Note that it is seen from Table 4 that, in particular, there exist strong correlations between $E_{\rm CEN}$ and the incompressibility coefficient $K_{\rm NM}$ for the ISGMR, between $E_{\rm CEN}$ and the effective mass m^*/m for the ISGQR and between $E_{\rm CEN}$ and the enhancement coefficient κ for the IVGDR EWSR and, surprisingly, very weak correlations between $E_{\rm CEN}$ and the symmetry energy J or its first and second derivative, for the IVGDR.

Table 4. **Pearson linear correlation coefficients between the centroid energy of each giant resonance and each nuclear matter property at saturation density (see Ref. [8])**

	$K_{\rm NM}$	J	L	$K_{\rm sym}$	m^*/m	κ
ISGMR	0.87	–0.10	0.25	0.45	–0.51	0.13
ISGDR	0.52	–0.10	0.13	0.36	–0.88	0.55
ISGQR	0.41	–0.09	0.15	0.41	–0.93	0.54
ISGOR	0.42	–0.10	0.15	0.43	–0.96	0.56
IVGMR	0.23	–0.26	–0.12	0.00	–0.70	0.86
IVGDR	0.05	–0.37	–0.42	–0.30	–0.60	0.84
IVGQR	0.18	–0.35	–0.29	–0.13	–0.74	0.80
IVGOR	0.25	–0.32	–0.19	0.02	–0.83	0.81

Fig. 4 shows the $E_{\rm CEN}$ of the ISGMR as a function $K_{\rm NM}$ of the corresponding Skyrme interaction used in the calculation. Each nucleus is plotted separately, and the appropriate experimental band is contained by the dashed lines. Overall we see the well-known strong correlation between the $E_{\rm CEN}$ and $K_{\rm NM}$ [7, 56], with a Pearson linear correlation coefficient $C \sim 0.87$ for all nuclei. It is interesting to note that we find a very weak correlation between $K_{\rm NM}$ and the $E_{\rm CEN}$ of the other compression modes, the ISGDR or the IVGMR (see Table 1). Fig. 5 shows the $E_{\rm CEN}$ of the ISGQR as a function of the effective mass m^*/m. We find a strong correlation between $E_{\rm CEN}$ and m^*/m (Pearson correlation coefficient $C = -0.93$). Fig. 6 shows the $E_{\rm CEN}$ of the IVGDR as a function of κ. We find a strong correlation between the values of the $E_{\rm CEN}$ and κ (Pearson correlation coefficient $C = 0.84$). As shown in Table 4 we find a very weak correlation between the values of the $E_{\rm CEN}$ of IVGDR and J $(C = -0.37)$, and similarly for its first derivative L $(C = -0.42)$ and second derivative $K_{\rm sym}$ $(C = -0.30)$. See Ref. [8] for other giant resonances.

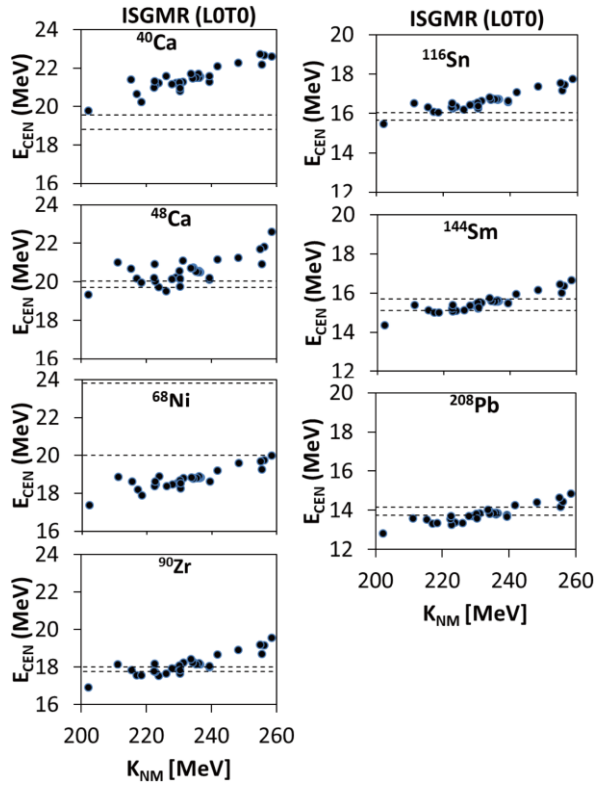

Fig. 4. Calculated centroid energies E_{CEN} in MeV (full circle) of the ISGMR for the different 33 Skyrme interactions (see section 3.5), as a function of the incompressibility coefficient K_{NM}. Each nucleus has its panel and the experimental uncertainties are contained by the dashed lines (Taken from Ref. [8]).

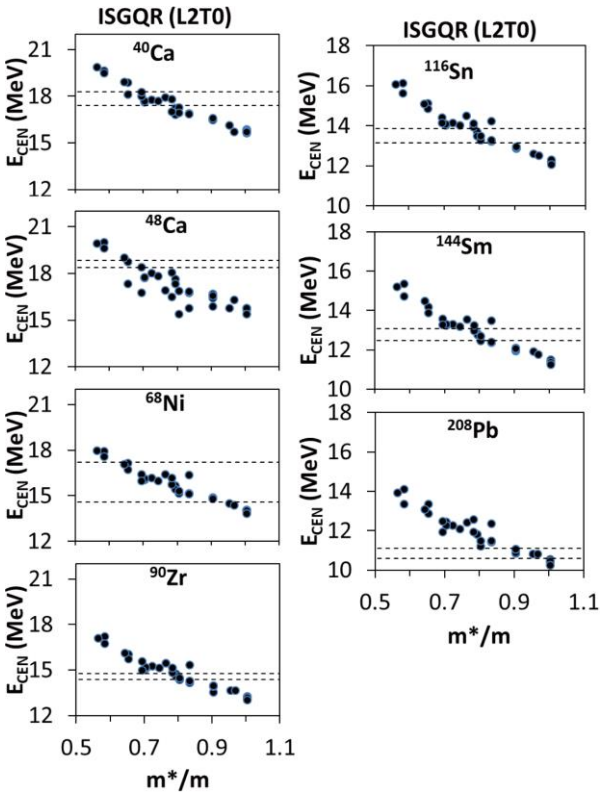

Fig. 5. Similar to Fig. 4, for the ISGQR as a function of the effective mass m^{*}/m (taken from Ref. [8]).

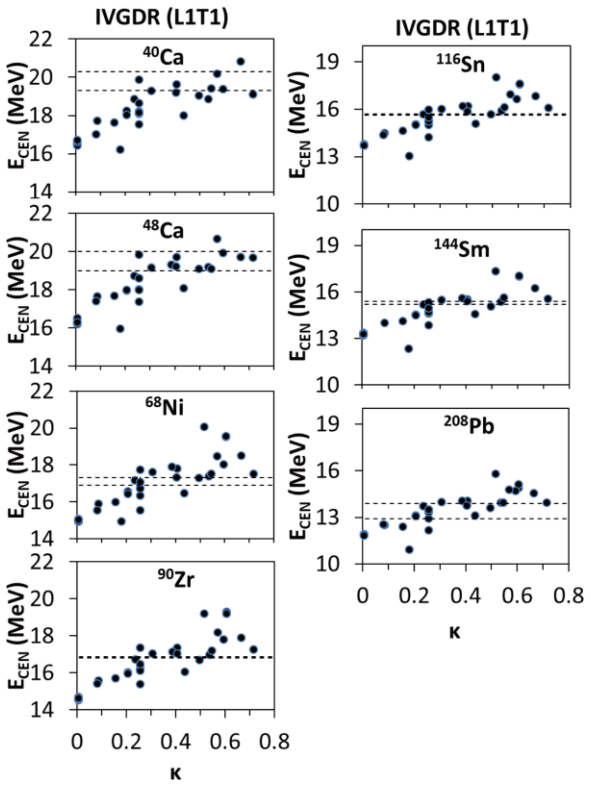

Fig. 6. Similar to Fig. 4, for the IVGDR as a function of the enhancement coefficient, κ, of the EWSR (Taken from Ref. [8]).

4. Summary and conclusions

We first described our knowledge of properties of isoscalar and isovector giant resonances of multipolarity $L = 0-3$, such as the strength functions $S(E)$ and centroid energies E_{CEN} and their sensitivities to bulk properties of NM. We then reviewed the current status of determining the parameters of modern EDF, associated with the standard form of the Skyrme type effective NN interaction, having ten (10) parameters. In section 2 we have presented a summary of the formalism of carrying out HF calculations of properties of ground states of nuclei, the formalism of carrying out HF-based RPA calculations of $S(E)$ and E_{CEN} and the FM) DWBA method for calculating the excitation cross-section of giant resonance by inelastic scattering with a projectile such as the α particle.

The results of our calculations were presented and discussed in section 3. We first describe the common approach employed in determining the parameters of the Skyrme interaction by a fit of HF results of properties of nuclei to experimental data, including constraints on NM properties. For example, the recent KDE0v1 was determined by a fit to binding energies and charge root-mean-square (rms) radii of nuclei ranging from the normal to exotic (proton- or neutron-rich) ones, and rms radii for $1d_{5/2}$ and $1f_{7/2}$ valence neutron orbits in the ^{17}O and ^{41}Ca nuclei,

respectively. We have included in the fit the experimental data on the constraint energies of the ISGMR and on the critical density $\rho_{cr} > 2\rho_0$, determined by the Landau parameters stability condition. Also included in the fit the constraints: (i) the slope of the symmetry energy must be positive for densities up to $3\rho_0$; (ii) the enhancement factor κ, of the EWSR for the IVGDR, should lie in the range of 0.1 to 0.5; and (iii) the Landau parameter G_0' of the particle-hole interaction, crucial for the spin properties of finite nuclei and nuclear matter, should be positive at $\rho = \rho_0$. We note that out of 240 Skyrme interactions, investigated by other researchers for the predictive power of these interactions, only the KDE0v1 also reproduce data on neutron stars and fission barriers that were not included in the fit. For comparison, we presented in Table 1 the parameters and the associated bulk properties of NM of the popular Skyrme interactions, SkM*, SLy4 and KDE0v1.

We also presented results of HF-based RPA calculations of $S(E)$ and E_{CEN}. We first considered problems of self-consistency in the calculations of $S(E)$ and E_{CEN}, the result of microscopic calculation of excitation cross-section of giant resonances needed for reliable determination of NM properties and demonstrated the model independence in deducing the incompressibility coefficient K_{NM} from the ISGMR E_{CEN}, obtained using the HF-based RPA in non-relativistic or relativistic models approaches. We then presented results of E_{CEN} and studied the sensitivities of E_{CEN} to bulk properties of NM by employing 33 Skyrme type interactions, commonly used in the literature. We have demonstrated:

(i) the important effects of violation of self-consistencies (SC) in HF-based RPA calculations of strength functions of giant resonances of multipolarities $L = 0-3$ and pointed out that due to a violation of SC the shift in the centroid energy of the ISGMR can be larger than 1 MeV (five times the experimental uncertainty), resolving the apparent dependence on the effective interactions in deducing K_{NM} from the ISGMR;

(ii) by carrying out highly accurate microscopic calculations of excitation cross-sections of the ISGMR and ISGDR and pointing out the missing strength at high excitation energy in the experimental measurement of the alpha excitation cross-section of the ISGDR. This was confirmed by more accurate experiment, resolving the disagreement in the value of K_{NM} deduced from the ISGMR or the ISGDR;

(iii) by constructing Skyrme interactions with values of K_{NM} similar to those obtained in the relativistic models we resolved the apparent model dependence in deducing the value of K_{NM} from the E_{CEN} of the ISGMR.

We have also presented results calculations of E_{CEN}, of the isoscalar $(T = 0)$ and isovector $(T = 1)$ giant resonances of multipolarities $L = 0-3$ in ^{40,48}Ca, ^{68}Ni, ^{90}Zr, ^{116}Sn, ^{144}Sm, and ^{208}Pb, within the fully self-consistent spherical HF-based RPA theory, using 33 different Skyrme-type effective NN interactions of the standard form commonly adopted in the literature. We reproduced the data for the E_{CEN} of the ISGMR, ISGQR, and IVGDR for most of the nuclei considered. For the ISGDR and ISGOR, we found that most of the interactions are consistently higher than the experimental values for the centroid energy. We also studied the sensitivity of E_{CEN} to bulk properties of nuclear matter (NM), such as the effective mass m^*/m, nuclear matter incompressibility coefficient K_{NM}, enhancement coefficient κ of the EWSR for the IVGDR and the symmetry energy J and its first L and second K_{sym} derivatives at saturation density, associated with the Skyrme interactions used in the calculations. By comparing the calculated values of E_{CEN} to the experimental data, we deduced constraints on the values of K_{NM}, m^*/m, and κ. We thus summarize our findings and conclude that:

– It is important to carry out fully self-consistent HF-based RPA calculations of E_{CEN} to deduced model-independent values for bulk properties of NM, in particular for the value of K_{NM}.

– It is important to carry out a very sensitive measurement of the excitation cross-section to deduce consistent values for bulk properties of NM from various giant resonances, particularly, for the K_{NM} from the E_{CEN} of the ISGMR and the ISGDR.

– We obtained strong, weak, and no correlations between the calculated values of E_{CEN} and K_{NM}, for the compression modes of the ISGMR $(C \sim 0.87)$, ISGDR $(C \sim 0.52)$ and the IVGMR $(C \sim 0.23)$, respectively.

– We obtained strong correlations between the effective mass m^*/m and the calculated values of E_{CEN} for the ISGDR $(C \sim -0.88)$, ISGQR $(C \sim -0.93)$, ISGOR $(C \sim -0.96)$ and IVGOR $(C \sim -0.83)$ and medium correlations for the IVGMR $(C \sim -0.70)$, IVGDR $(C \sim -0.60)$, and IVGQR $(C \sim -0.74)$.

We obtained strong correlations between the calculated values of the E_{CEN} and the enhancement

coefficient, κ, for the EWSR of the IVGDR for all the isovector giant resonances considered $(C = 0.80 - 0.86)$.

– We found weak to no correlations between the calculated values of E_{CEN} and the symmetry energy coefficients J, L or K_{sym} for all the isovector resonances considered, see Table 4 for details.

– Considering the results of the E_{CEN} of the ISGMR, ISGQR, and IVGDR of ^{40,48}Ca, ^{68}Ni, ^{90}Zr, ^{116}Sn, ^{144}Sm and ^{208}Pb we find that the interactions associated with NM properties in the following range best reproduce the experimental data: $K_{\mathrm{NM}} = 210 - 240$ MeV, $m^*/m = 0.7 - 0.9$ and $\kappa = 0.25 - 0.70$.

We add that the constraints on NM properties that we obtained can be used to develop the next generation of EDF by imposing the constraints in the fits used to determine the values of the parameters of the Skyrme interaction. We note that although these constraints may depend on the specific form of the interaction adopted, it is known that the centroid energy of the ISGMR is sensitive to K_{NM}. Similarly, the ISGQR is sensitive to the value of m^*/m [57] because the effective mass influences the spacing between major nuclear shells and therefore the distribution of the response function. We also point out that when determining the best range for the effective mass we emphasized the results of the heavier nuclei more. Lastly, the dependence of the centroid energy of the IVGDR on κ, is expected from Eq. (22) for the EWSR of the IVGDR, which is given by constant times $(1+\kappa)$.

This work is dedicated to our longtime friend and collaborator, Academician Professor Volodymyr M. Kolomietz who died in June 2018, a personal loss to us and his family. S.S. is supported in part by the US Department of Energy, under Grant No DE-FG03-93ER40773. A.I.S. is partially supported by the Fundamental Research program "Fundamental research in high energy physics and nuclear physics (international collaboration)" of the National Academy of Sciences of Ukraine.

REFERENCES

1. W. Kohn. Nobel Lecture: Electronic structure of matter – wave functions and density functionals. Rev. Mod. Phys. 71 (1999) 1253.
2. N.K. Glendenning. Equation of state from nuclear and astrophysical evidence. Phys. Rev. C 37 (1988) 2733.
3. J.M. Lattimer, M. Prakash. Neutron star observations: Prognosis for equation of state constraints. Phys. Rep. 442 (2007) 109.
4. A. Bohr, B.M. Mottelson. *Nuclear Structure II* (New York: Benjamin, 1975).
5. V.M. Kolomietz, S. Shlomo. *Mean Field Theory* (Singapore: World Scientific, 2020) 565 p.
6. S. Shlomo, D.H. Youngblood. Nuclear matter compressibility from isoscalar giant monopole resonance. Phys. Rev. C 47 (1993) 529.
7. S. Shlomo. Modern Energy Density Functional for Nuclei and the Nuclear Matter Equation of State. In: *The Universe Evolution: Astrophysical and Nuclear Aspects.* Eds. I. Strakovsky, L. Blokhintsev (New York: Nova Science Publishers, 2013) p. 323.
8. G. Bonasera, M.R. Anders, S. Shlomo. Giant resonances in ^{40,48}Ca, ^{68}Ni, ^{90}Zr, ^{116}Sn, ^{144}Sm, and ^{208}Pb. Phys. Rev. C 98 (2018) 054316.
9. B.K. Agrawal, S. Shlomo, V. Kim Au. Determination of the parameters of a Skyrme type effective interaction using the simulated annealing approach. Phys. Rev. C 72 (2005) 014310.
10. M. Bender, P.-H. Heenen, P.-G. Reinhard. Self-consistent mean-field models for nuclear structure. Rev. Mod. Phys. 75 (2003) 121.
11. Takashi Nakatsukasa et al. Time-dependent density-functional description of nuclear dynamics. Rev. Mod. Phys. 88 (2016) 045004.
12. X. Roca-Maza, N. Paar. Nuclear equation of state from ground and collective excited state properties of nuclei. Prog. Part. Nucl. Phys. 101 (2018) 96.
13. D. Vautherin, D.M. Brink. Hartree-Fock Calculations with Skyrme's Interaction. I. Spherical Nuclei. Phys. Rev. C 5 (1972) 626.
14. T.H.R. Skyrme. CVII. The Nuclear Surface. Phil. Mag. 1 (1956) 1043.
15. T.H.R. Skyrme. The effective nuclear potential. Nucl. Phys. 9 (1959) 615.
16. M. Dutra et al. Skyrme interaction and nuclear matter constraints. Phys. Rev. C 85 (2012) 035201; P.D. Stevenson et al. Do Skyrme forces that fit nuclear matter work well in finite nuclei? arXiv:1210.1592 [nucl-th].
17. E. Chabanat et al. A Skyrme parametrization from subnuclear to neutron star densities. Nucl. Phys. A 627 (1997) 710; A Skyrme parametrization from subnuclear to neutron star densities Part II. Nuclei far from stabilities. Nucl. Phys. A 635 (1998) 231.
18. S. Shlomo, G.F. Bertsch. Nuclear response in the continuum. Nucl. Phys. A 243 (1975) 507.
19. Tapas Sil et al. Effects of self-consistency violation in Hartree-Fock RPA calculations for nuclear giant resonances revisited. Phys. Rev. C 73 (2006) 034316.
20. B.K. Agrawal, S. Shlomo, A.I. Sanzhur. Self-cosistent Hartree-Fock based random phase approximation and the spurious state mixing. Phys. Rev. C 67 (2003) 034314.

21. S. Shlomo, A.I. Sanzhur. Isoscalar giant dipole resonance and nuclear matter incompressibility coefficient. Phys. Rev. C 65 (2002) 044310.
22. P.-G. Reinhard. From sum rules to RPA: 1. Nuclei. Ann. Phys. 504 (1992) 632.
23. G.R. Satchler. *Direct Nuclear Reactions* (Oxford: Oxford University Press, 1983).
24. A. Kolomiets, O. Pochivalov, S. Shlomo. Microscopic description of excitation of nuclear isoscalar giant resonances by inelastic scattering of 240 MeV α-particles. Phys. Rev. C 61 (2000) 034312.
25. M.H. MacFarlane, S.C. Pieper. PTOLEMY: A program for heavy-ion direct-reaction calculations. Argonne National Laboratory report No. ANL-76-11, Rev. 1 (1978) 104 p. (unpublished).
26. S. Shlomo. Compression modes and the nuclear matter incompressibility coefficient. Pramana - J. Phys. 57 (2001) 557.
27. S. Shlomo, V.M. Kolomietz, B.K. Agrawal. Isoscalar giant monopole resonance and its overtone in microscopic and macroscopic models. Phys. Rev. C 68 (2003) 064301.
28. B.K. Agrawal, S. Shlomo, V. Kim Au. Critical densities for the Skyrme type effective interactions. Phys. Rev. C 70 (2004) 057302.
29. J. Bartel et al. Towards a better parametrization of Skyrme-like effective forces: a critical study of the SkM force. Nucl. Phys. A 386 (1982) 79.
30. S. Shlomo. Nuclear Coulomb energies. Rep. Prog. Phys. 41 (1978) 957.
31. S. Shlomo. Coulomb energies and charge asymmetry of nuclear forces. Phys. Lett. B 42 (1972) 146.
32. S. Shlomo, D.O. Riska. Charge symmetry breaking interactions and coulomb energy differences. Nucl. Phys. A 254 (1975) 281.
33. S. Shlomo, W.G. Love. Core Polarization and Coulomb Displacement Energies. Physica Scripta 26 (1982) 280.
34. J. Button et al. Isoscalar $E0$, $E1$, $E2$ and $E3$ strength in ^{94}Mo. Phys. Rev. C 94 (2016) 034315.
35. B.K. Agrawal, S. Shlomo. Consequences of self-consistency violations in Hartree-Fock random-phase approximation calculations of the nuclear breathing mode energy. Phys. Rev. C 70 (2004) 014308.
36. N.V. Giai, H. Sagawa. Spin-isospin and pairing properties of modified Skyrme interactions. Phys. Lett. B 106 (1981) 379.
37. H.P. Morsch et al. New Giant Resonances in 172-MeV α Scattering from ^{208}Pb. Phys. Rev. Lett. 45 (1980) 337.
38. K.-F. Liu et al. Skyrme-Landau parameterization of effective interactions (I). Hartree-Fock ground states. Nucl. Phys. A 534 (1991) 1; Skyrme-Landau parameterization of effective interactions (II). Self-consistent description of giant multipole resonances. Nucl. Phys. A 534 (1991) 25.
39. N.V. Giai, H. Sagawa. Monopole and dipole compression modes in nuclei. Nucl. Phys. A 371 (1981) 1.
40. D.H. Youngblood et al. Isoscalar $E0$-$E3$ strength in ^{116}Sn, ^{144}Sm, ^{154}Sm, and ^{208}Pb. Phys. Rev. C 69 (2004) 034315.
41. G.A. Lalazissis, J. König, P. Ring. New parametrization for the Lagrangian density of relativistic mean field theory. Phys. Rev. C 55 (1997) 540.
42. B.K. Agrawal, S. Shlomo, V. Kim Au. Nuclear matter incompressibility coefficient in relativistic and nonrelativistic microscopic models. Phys. Rev. C 68 (2003) 031304.
43. D.H. Youngblood et al. Compression mode resonances in ^{90}Zr. Phys. Rev. C 69 (2004) 054312.
44. P.-G. Reinhard, H. Flocard. Nuclear effective forces and isotope shifts. Nucl. Phys. A 584 (1995) 467.
45. K. Klüpfel et al. Variations on a theme by Skyrme: A systematic study of adjustments of model parameters. Phys. Rev. C 79 (2009) 034310.
46. N. Lyutorovich et al. Self-consistent calculations of the electric giant dipole resonances in light and heavy nuclei. Phys. Rev. Lett. 109 (2012) 092502.
47. L. Bennour et al. Charge distribution of ^{208}Pb, ^{206}Pb, and ^{205}Tl and the mean-field approximation. Phys. Rev. C 40 (1989) 2834.
48. P.-G. Reinhard et al. Shape coexistence and the effective nucleon-nucleon interaction. Phys. Rev. C 60 (1999) 014316.
49. L.G. Cao et al. From Brueckner approach to Skyrme-type energy density functional. Phys. Rev. C 73 (2006) 014313.
50. L.-W. Chen et al. Density slope of the nuclear symmetry energy from neutron skin thickness of heavy nuclei. Phys. Rev. C 82 (2010) 024321.
51. A.W. Steiner et al. Isospin asymmetry in nuclei and neutron stars. Phys. Rep. 411 (2005) 325.
52. P.A.M. Guichon et al. Physical origin of density dependent forces of Skyrme type within the quark meson coupling model. Nucl. Phys. A 772 (2006) 1.
53. F. Tondeur et al. Static nuclear properties and the parametrization of Skyrme forces. Nucl. Phys. A 420 (1984) 297.
54. B.A. Brown et al. Neutron skin deduced from antiprotonic atom data. Phys. Rev. C 76 (2007) 034305.
55. J. Friedrich, P.-G. Reinhard. Skyrme-force parameterization: Least-squares fit to nuclear ground-state properties. Phys. Rev. C 33 (1986) 335.
56. S. Shlomo, V.M. Kolomietz, G. Colò. Deducing the nuclear-matter incompessibility coefficient from data on isoscalar compression modes. Eur. Phys. J. A 30 (2006) 23.
57. M. Golin, L. Zamick. Collective models of giant states with density dependent interactions. Nucl. Phys. A 249 (1975) 320.

Ш. Шломо[1], А. І. Санжур[2,*]

[1] Циклотронний інститут, Техаський A&M університет, Коледж Стейшн, США
[2] Інститут ядерних досліджень НАН України, Київ, Україна

*Відповідальний автор: sanjour@kinr.kiev.ua

ФУНКЦІОНАЛ ГУСТИНИ ЕНЕРГІЇ ТА ЧУТЛИВІСТЬ ЕНЕРГІЙ ГІГАНТСЬКИХ РЕЗОНАНСІВ ДО ВЛАСТИВОСТЕЙ ЯДЕРНОЇ МАТЕРІЇ

Запропоновано короткий огляд поточного стану ядерного функціоналу густини енергії та теоретичних результатів, отриманих для ядер і ядерної матерії. Описано метод визначення параметрів функціонала густини енергії, пов'язаного з ефективною взаємодією Скірма, шляхом підгонки на основі теорії Хартрі - Фока (HF) до широкого набору даних по властивостях основних станів ядер з урахуванням відповідних обмежень. Далі описано основане на теорії HF повністю самоузгоджене наближення випадкових фаз (RPA) для розрахунку силових функцій $S(E)$ і середніх енергій (центроїдів) E_{CEN} гігантських резонансів і борнівське наближення спотворених хвиль (DWBA) на основі моделі згортки (FM) для обчислення перерізів збуджень гігантських резонансів при розсіянні α-частинок. Наведено такі результати: параметри Скірма функціонала густини енергії KDE0v1; наслідки порушення самоузгодженості RPA на основі HF; розрахунки перерізів збудження за допомогою FM-DWBA; значення E_{CEN} ізоскалярного та ізовекторного гігантських резонансів мультипольності $L=0-3$ для широкого кола сферичних ядер із застосуванням 33 функціоналів густини енергії на основі стандартної форми взаємодії Скірма, що зазвичай використовується в літературі; чутливість E_{CEN} гігантських резонансів до основних властивостей ядерної матерії. Визначено також обмеження на такі властивості ядерної матерії, як нестисливість і ефективна маса нуклона, порівнюючи розрахунки з експериментальними даними по E_{CEN} гігантських резонансів.

Ключові слова: функціонал густини енергії, гігантський резонанс, ядерна матерія, силова функція, наближення випадкових фаз.

Ш. Шломо[1], А. И. Санжур[2,*]

[1] Циклотронный институт, Техасский A&M университет, Колледж Стейшн, США
[2] Институт ядерных исследований НАН Украины, Киев, Украина

*Ответственный автор: sanjour@kinr.kiev.ua

ФУНКЦИОНАЛ ПЛОТНОСТИ ЭНЕРГИИ И ЧУВСТВИТЕЛЬНОСТЬ ЭНЕРГИЙ ГИГАНТСКИХ РЕЗОНАНСОВ К СВОЙСТВАМ ЯДЕРНОЙ МАТЕРИИ

Представлен краткий обзор текущего статуса ядерного функционала плотности энергии и теоретических результатов, полученных для ядер и ядерной материи. Описан метод определения параметров функционала плотности энергии, связанного с эффективным взаимодействием Скирма с помощью подгонки на основе теории Хартри - Фока (HF) к широкому набору данных по свойствам основных состояний ядер, с учетом соответствующих ограничений. Далее описано основанное на теории HF полностью самосогласованное приближение случайных фаз (RPA) для расчета силовых функций $S(E)$ и средних энергий (центроидов) E_{CEN} гигантских резонансов и борновское приближение искаженных волн (DWBA) на основе модели свертки (FM) для расчета сечений возбуждения гигантских резонансов при рассеянии α-частиц. Приведены следующие результаты: параметры Скирма функционала плотности энергии KDE0v1; последствия нарушения самосогласованности RPA на основе HF; расчеты сечений возбуждения с помощью FM-DWBA; значения E_{CEN} изоскалярного и изовекторного гигантских резонансов с мультипольностью $L=0-3$ для широкого набора сферических ядер, применяя 33 функционала плотности энергии стандартной формы сил Скирма, которая обычно используется в литературе; чувствительность E_{CEN} гигантских резонансов к изменениям основных свойств ядерной материи. Определены также ограничения на такие свойства ядерной материи, как несжимаемость и эффективная масса нуклона, путем сравнения расчетов с экспериментальными данными по E_{CEN} гигантских резонансов.

Ключевые слова: функционал плотности энергии, гигантский резонанс, ядерная материя, силовая функция, приближение случайных фаз.

Надійшла/Received 12.11.2019